Toxicology in Vitro 65 (2020) 104757

Contents lists available at ScienceDirect

Toxicology in Vitro

journal homepage: www.elsevier.com/locate/toxinvit

In vitro and bioinformatics mechanistic-based approach for cadmium carcinogenicity understanding

Monica Oldani[a], Marco Fabbri[b], Pasquale Melchioretto[c], Giulia Callegaro[c,d], Paola Fusi[a,f], Laura Gribaldo[e,*], Matilde Forcella[a,1], Chiara Urani[c,f,1]

[a] Department of Biotechnology and Biosciences, University of Milan – Bicocca, Piazza della Scienza 3, 20126 Milan, Italy
[b] Dana-Farber Cancer Institute, 450 Brookline Ave, Boston, MA 02215, USA
[c] Department of Earth and Environmental Sciences, University of Milan – Bicocca, Piazza della Scienza 1, 20126 Milan, Italy
[d] Division of Drug Discovery and Safety, Leiden Academic Centre for Drug Research (LACDR), Leiden University, The Netherlands
[e] European Commission, DG Joint Research Centre, Via Fermi 2749, 21027 Ispra, VA, Italy
[f] Integrated Models for Prevention and Protection in Environmental and Occupational Health, (MISTRAL) Interuniversity Research Center, Italy

ARTICLE INFO

Keywords:
Cadmium
Carcinogenesis
Cell transformation assay
Toxicogenomics

ABSTRACT

Cadmium is a toxic metal able to enter the cells through channels and transport pathways dedicated to essential ions, leading, among others, to the dysregulation of divalent ions homeostasis. Despite its recognized human carcinogenicity, the mechanisms are still under investigation. A powerful tool for mechanistic studies of carcinogenesis is the Cell Transformation Assay (CTA). We have isolated and characterized by whole genome microarray and bioinformatics analysis of differentially expressed genes (DEGs) cadmium-transformed cells from different *foci* (F1, F2, and F3) at the end of CTA (6 weeks). The systematic analysis of up- and down-regulated transcripts and the comparison of DEGs in transformed cells evidence different functional targets and the complex picture of cadmium-induced transformation. Only 34 in common DEGs are found in cells from all *foci*, and among these, only 4 genes are jointly up-regulated (*Ccl2*, *Ccl5*, *IL6* and *Spp1*), all responsible for cytokines/chemokines coding. Most in common DEGs are down-regulated, suggesting that the switching-off of specific functions plays a major role in this process. In addition, the comparison of dysregulated pathways immediately after cadmium treatment with those in transformed cells provides a valuable means to the comprehension of the overall process.

1. Introduction

Cadmium (Cd) is a toxic metal massively released into the environment (~30,000 tons/year) due to anthropogenic activities. Besides occupational exposure, Cd contamination in humans can occur through food, drinking water, inhalation of air particles, and cigarette smoking. It has been estimated that daily intake of Cd from food is generally between 8 and 25 μg (Jarup and Akesson, 2009). Cadmium ions (Cd^{2+}) enter the cells through channels and transport pathways dedicated to essential ions, in what has been named a "Trojan horse mechanism" (Martelli et al., 2006). Once absorbed, Cd is trapped in the body and evades detoxification leading to an estimated biological half-life of > 26 years. The accumulation of this metal contributes to the increase of oxidative stress and to the alteration of divalent ions homeostasis, primarily Zn^{2+} and Ca^{2+} (Choong et al., 2014); (Thevenod, 2010); (Urani et al., 2015); (Callegaro et al., 2018). Notably, about 3200 proteins (~10% of the human proteome) require zinc to properly function, and, along with the ability of Cd to replace Zn in zinc-finger regions or zinc-domains functionally important for many proteins and enzymes (Meplan et al., 1999); (Tang et al., 2014), these features suggest a role for Cd in essential metal dyshomeostasis, leading to alterations of physiological processes.

Cd is involved in global and site-specific DNA methylation, according to studies performed on model organisms (Hwang et al., 2019) as well as in humans (Ray et al., 2014). Cd-associated epigenetic effects have also been studied in the context of other exposures such as smoking (Virani et al., 2016). Last but not least, Cd is a well-known carcinogen as classified by the International Agency for Research on Cancer, but the mechanisms underpinning the molecular processes are not completely clarified.

* Corresponding author at: European Commission, Via Enrico Fermi 2749, 21027 Ispra, VA, Italy.
E-mail address: laura.gribaldo@ec.europa.eu (L. Gribaldo).
[1] Matilde Forcella and Chiara Urani are joint Senior Authors.

https://doi.org/10.1016/j.tiv.2020.104757
Received 18 September 2019; Received in revised form 28 November 2019; Accepted 1 January 2020
Available online 03 January 2020
0887-2333/

Cadmium carcinogenicity has been well demonstrated both in *in vitro* biological systems (Urani et al., 2009; Ao et al., 2010), such as the Cell Transformation Assays (CTAs), and in humans and animal models (Hartwig, 2013). The CTA is the most advanced *in vitro* assay for human carcinogenicity prediction induced by chemicals (Vanparys et al., 2012). It has been shown to closely model some *in vivo* key stages of the conversion of normal cells into malignant ones, and it is a powerful tool for mechanistic studies of carcinogenesis. Suitable cell lines are exposed to suspected carcinogens and, as a consequence of cell transformation, *foci* of transformed cells are formed after 3–6 weeks (OECD, 2007).

The CTA offers the unique advantage of studying in a standardized and controlled environment the signals that trigger chemical-induced carcinogenesis, and the biochemical processes and pathways deregulated in transformed cells (*foci)*. Furthermore, these assays are extremely important in the context of the 3Rs as they provide a means to reduce the use of animals, as CTA can be used to pre-screen for the potential of human carcinogens. Up to now, the use of alternative non-animal approaches, such as the CTA, in the context of carcinogenesis has been limited for different reasons, among which the lack of a complete comprehension of the carcinogenesis processes. Finally, even though the CTA should not be used as a stand-alone assay to predict carcinogenesis in the regulatory context, these assays are proposed as one of the building blocks in an integrated approach (Corvi and Madia, 2017; Corvi et al., 2017), thus stressing their importance in mechanistic studies and in hazard assessment.

The aim of this work is to investigate, through a toxicogenomic approach based on whole genome microarray analysis of gene expression and on a bioinformatics study, the differentially regulated genes in transformed cells from different *foci* obtained at the end of the *in vitro* cell transformation upon exposure of C3H10T1/2 cells to the same stimulus (1 μM $CdCl_2$ 24 h treatment). The systematic analysis of deregulated genes and pathways in transformed cells, along with the comparison to what has previously been obtained by our group after the analysis of early responses to $CdCl_2$ exposure in the same cell model (Forcella et al., 2016; Callegaro et al., 2018), will provide a picture of triggering signals, of specific signatures and mechanistic processes in cadmium-induced cell transformation. Furthermore, these methods could represent a step forward in the development of a mechanistic-based approach for carcinogenesis alternative methods.

2. Materials and methods

2.1. Cells and culture conditions

The experiments were performed using the cells collected from Cd-transformed *foci* obtained at the end of Cell Transformation Assays (CTAs) on C3H10T1/2 clone 8 mouse embryonic fibroblasts (cell line ATCC, CCL 226 lot. n. 58078542). This cell line was chosen for its high sensitivity to carcinogenic compounds, its low spontaneous transformation rates, and because it represents one of the three cell lines suggested in the Detailed Review Paper on Cell Transformation Assay to be used for detection of chemical carcinogens (OECD, 2007). Cells with passages from 9 to 12 were used for cell transformation studies (OECD, 2007).

C3H cells were seeded at a density of 800 cells/dish in 100 mm diameter Petri dishes, and exposed 24 h after seeding to 1 μM $CdCl_2$ for 24 h. Previous Cell Transformation Assays performed by our group (Urani et al., 2009) on a wide range of $CdCl_2$ concentrations demonstrated that 1 μM $CdCl_2$, which is below the cytotoxicity threshold (IC_{50} of 2.4 μM), is able to induce the formation of transformed *foci*. Samples treated with $CdCl_2$ were exposed 4 days after the treatment to 0.1 μg/ml TPA (12-O-tetradecanoylphorbol-13-acetate), a known tumour promoter, in DMSO. TPA addition was maintained throughout all the experiments. Cells exposed to 0.1 μg/ml TPA alone were used as reference control. After 24 h of treatment, the cells were rinsed twice with phosphate buffered saline (PBS) and fresh medium was added. The medium was changed weekly. Upon confluence (around the 3rd week), high serum (10% FBS) medium was substituted with low (5% FBS) serum medium. The samples were observed weekly under a light microscope throughout the duration of the assay (6 weeks) to check healthy cells' status and *foci* formation.

Different cell types were collected at the end of the CTAs, and the derived cell clones were cultured and processed for further analyses, as described in the following sections. The new cell clones were derived from three different fully transformed *foci,* all obtained after the initial exposure (24 h) to1 μM $CdCl_2$, and classified as F1, F2, and F3.

Cells were cultured in Basal Medium Eagle (BME, Sigma Chemical Co., St. Louis, MO, USA) enriched with 10% heat-inactivated foetal bovine serum (FBS, Euroclone, Pero, Italy), 1% glutamine, 0.5% HEPES 2 M and 25 μg/ml gentamicin (all purchased from Sigma) at 37 °C in a humidified incubator supplied with a constant flow of 5% CO_2 in air throughout each experiment. Cells were routinely seeded in 100 mm Ø Petri dishes, the medium was changed every 3 days and cells grown until 80% confluence maximum was reached. The cells were stored in ampoules, frozen at −80 °C with 10% sterile DMSO as a preservative.

2.2. RNA extraction and purification

All cell clones were harvested by trypsinization at 80% confluence and lysed in 300 μl RLT buffer (Qiagen, Germantown, MD, USA), with 1:100 β-mercaptoethanol added. Homogenates were obtained by passing 5 times through a blunt 20-gauge needle fitted to a syringe. Samples were stored at −80 °C until RNA extraction was carried out.

RNA was purified from cell clones using the RNeasy Plus kit (Qiagen, Germantown, MD, USA). RNA was quantified using a ND-1000 UV–Vis Spectrophotometer (NanoDrop Technologies), and RNA integrity was assessed with the Agilent 2100 Bioanalyzer (Agilent), according to the manufacturer's instructions. RNA samples used in this study all had a 260/280 ratio above 1.9 and an RNA Integrity Number (RIN) above 9.0.

2.3. Microarray expression profiling and exploratory statistical analyses of the three foci

In the microarray experiments, all sample-labelling, hybridization, washing, and scanning steps were conducted following the manufacturer's specifications. In brief, Cy3-labeled cRNA was generated from 500 ng input total RNA using Quick Amp Labeling Kit, One-colour (Agilent).

For every sample, 1.65 μg cRNA from each labelling reaction (with a specific activity above 9.0) was hybridized using the Gene Expression Hybridization Kit (Agilent) to the SurePrint G3 Mouse GE 8x60K Microarray (G4852, Agilent), which is an 8 × 60 k 60mer slide format. After hybridization, the slides were washed and then scanned with the Agilent G2565BA Microarray Scanner (Agilent). The fluorescence intensities on scanned images were extracted and pre-processed by Agilent Feature Extraction Software (v10.5.1.1). Quality control and array normalization was performed in the R statistical software environment using the Agi4x44PreProcess package downloaded from the Bioconductor web site (Gentleman et al., 2004). The normalization and filtering steps were based on those described in the Agi4x44PreProcess reference manual.

In order to detect differences in gene expression among different cell populations a moderate *t*-test was applied. Moderated *t* statistics were generated by the Limma Bioconductor package. Modulated genes were chosen as those with a fold change > 1 or smaller than −1 and a false discovery rate (Benjamini and Hochberg's method) corrected *p*-value smaller than 0.05 (Smyth, 2004).

2.4. Quantitative real time-PCR

RNA was reverse-transcribed using SuperScript® II RT (Invitrogen,

Carlsbad, CA, USA), oligo dT and random primers, according to the manufacturer's protocol.

The SYBR Green method was used for quantitative real-time PCR (Q-PCR). Briefly, 50 ng cDNA was amplified with SYBR Green PCR Master Mix (Applied Biosystems, Foster City, CA, USA) and specific primers (100 nM), using an initial denaturation step at 95 °C for 10 min, followed by 40 cycles of 95 °C for 15 s and 59 °C annealing for 1 min. Each sample was analyzed for Interleukin 6 expression and normalized for total RNA content using β-actin gene as an internal reference control. The relative expression level was calculated with the Livak method (2[-ΔΔC(T)]) (Livak and Schmittgen, 2001) and was expressed as a fold change ± standard deviation. The accuracy was monitored by the analysis of melting curves. The following primers were used: Interleukin 6 Fw 5′-AGCCAGAGTCCTTCAGAGAGA-3′ and Rv 5′-TGGTCTT GGTCCTTAGCCAC-3′; β-actin Fw 5′-CCACCATGTACCCAGGCATT-3′ and Rv 5′-CGGACTCATCGTACTCCTGC-3′.

2.5. Functional enrichment analysis

Differentially Expressed Genes (DEGs), namely up-regulated and down-regulated genes, were analyzed with WebGestalt (WEB-based Gene SeT AnaLysis Toolkit, http://www.webgestalt.org), to identify genes with similar functions (Wang et al., 2013). Enrichment analyses were conducted studying the Gene Ontology categories with a *p*-value lower than 0.05 in a hypergeometric test. The method used for enrichment analysis was the Over-Representation Analysis (ORA). WebGestalt gene tables summarization and volcano plots were used to summarize and visualize the enrichment results.

3. Results

One of the purposes of the study was the identification of specific transcriptomic signatures able to unravel cadmium-induced carcinogenesis. In this regard, cDNA microarrays were used to analyze the modulation of gene expression induced by 1 μM cadmium chloride ($CdCl_2$) at the end of Cell Transformation Assay (CTA) (Callegaro et al., 2018), using TPA-treated cells as a reference control. Thus, we performed a systematic analysis of the functions of up- and down-regulated genes in cells derived from three *foci* (F1, F2, and F3) to figure out a picture of cadmium promoted pathogenic mechanisms leading to cells transformation.

3.1. Differentially expressed genes (DEGs) in F1 focus

Among the top 15 up-regulated genes in F1 *focus*, listed in Table 1, we found a series of genes involved in inflammation, such as *Cfh* gene coding for complement factor H, a major regulator of the alternative pathway of the complement system, which is able to bind neutrophiles, macrophages and monocytes with a proinflammatory effect (Jozsi et al., 2018). In addition, through a function not related to its complement-regulatory capacity, receptor-bound factor H can mediate or regulate cell adhesion.

Another gene involved in inflammation is *Spp1* gene coding for Osteopontin (also known as optineurin), a cytokine and cell attachment phosphoprotein expressed by various tissues and cell types and involved in multiple functions such as inflammation, cell adhesion, migration and tumour invasion. In particular, osteopontin is known to up-regulate MMP-2 expression and activity in tumour cells (Zhang et al., 2011) and may act as a potent angiogenic factor (Zhao et al., 2018). Another transcript related to inflammation is the T-cell specific GTPase 2 isoform X1, coded by *Tgtp2*, which has been demonstrated to be involved in systemic inflammatory response syndrome (SIRS) (Mastronardi et al., 2007), as well as in antiviral response (Carlow et al., 1998).

Lumican, coded by up-regulated *Lum* gene, is a member of the small leucine-rich proteoglycan family, expressed in the extracellular matrix of different tissues, where it plays a critical role in collagenous matrix assembly, protecting collagen from cleavage by matrix metalloproteinase-9 (MMP-9) (Malinowski et al., 2012). Its ability to down-regulate the proteolytic activity associated with endothelial cell membranes, particularly MMP-14 and MMP-9, gives Lumican angiostatic properties.

Other up-regulated genes code for proteins involved in cell proliferation, migration and invasion, like FBJ osteosarcoma oncogene B (coded by *Fosb* gene) which promotes cell survival, and Histone deacetylase (coded by *Hdac9* gene), a negative regulator of adipogenic differentiation, whose over-expression has been documented in several malignancies.

Capn6, encoding for Calpain 6 (CAPN6), was also found to be up-regulated in cells from F1 *focus*. Unlike the other members of the family, CAPN6 is not a proteolytic enzyme (Dear et al., 1997), since it lacks the active-site catalytic cysteine residue. Instead, it has been shown to modulate osteoclasts and stabilize microtubules (Tonami et al., 2011).

Among the 15 top down-regulated genes in cells from F1 *focus* (also listed in Table 1) we found *Rspo3* gene, a homolog of *Xenopus laevis R-spondin 3* gene. R-spondins (RSPO) are agonists of the Wnt pathway, interfering with the clearance of Wnt receptors from the plasma membrane (Fischer et al., 2017). RSPO3 expression has been shown to cause rapid development of adenoma and adenocarcinoma in the intestine, establishing RSPO3 as an efficient, causal driver of intestinal cancer (Hilkens et al., 2017).

Another interesting down-regulated gene, *Slc17a3*, coding for a member of solute carrier family 17 (sodium phosphate), isoform CRA_c.

Mest gene, which was down-regulated in cells from all the three *foci*, codes for mesoderm-specific transcript protein isoform 1 precursor (MEST), a putative alpha/beta hydrolase, although the substrate of this enzyme has not yet been identified (Kaneko-Ishino et al., 1995). A functional role related to oncofetal angiogenesis has been suggested for the MEST proteins (Mayer et al., 2000).

PEP-19/pcp4 is a neuron-specific peptide in the adult brain, binding to the C-domain of calmodulin; a role for PEP-19/pcp4 as a regulator of synaptic plasticity in the mouse striatum, in the context of spatial learning, has recently been proposed (Aerts et al., 2017).

Gas6 gene, coding for growth arrest specific 6 protein, was found to be down-regulated also in cells from F2 and F3 *foci*. Gas6 protein activates STAT3 signalling and stimulates the molecular process of differentiation or myelination in the adult optic nerve (Goudarzi et al., 2016). Moreover, other authors (Ray et al., 2017) found that the complete deletion of the Gas6 signalling pathway significantly impacted resolution of inflammation, axonal integrity and remyelination. Gas6 therefore seems to have an anti-inflammatory effect and a role in cell differentiation, its down-regulation likely leading to loss of differentiation and inflammation.

Slit3 gene, also down-regulated in F1 *focus*, codes for a member of the Slits proteins, large matrix proteins that are secreted by endothelial cells. Slit3 was reported to enhance monocyte migration *in vitro*, as well as myeloid cell recruitment *in vivo* and to induce the activation of RhoA, a member of the Rho family of small GTPases (Geutskens et al., 2010).

Mgmt gene codes for O-6-methylguanine-DNA methyltransferase (MGMT), a DNA alkyl transferase; a role in the development of certain kinds of human tumours is suggested by the observation that *Mgmt* gene is silenced by promoter methylation in gliomas, colorectal tumours, non-small-cell lung carcinoma, lymphomas and head and neck cancers (Mari-Alexandre et al., 2017).

Heparan sulfate 6-O-sulfotransferase 2 (HS6ST2), transcript variant 2, coded by *Hs6st2* gene, belongs to the HS6ST family, comprising different isoforms with distinct substrate preferences. HS6ST-1-deficiency is lethal to mice mostly at later embryonic stages, leading to various malformations in muscle development (Habuchi and Kimata, 2010).

Smpdl3a gene codes for sphingomyelin phosphodiesterase acid-like 3A (SMPDL3A), a di-zinc-dependent enzyme, which, in contrast to sphingomyelinase, is inactive against sphingomyelin and can instead

Table 1
List of top 15 up- and down-regulated genes in cells from F1 *focus*. DEGs are listed in descending order of fold change compared to TPA-treated cell clone.

GeneName	Description	Fold change
chr10:119960546-119979696_F	lincRNA: chr10:119960546-119979696 forward strand	12.34
Cfh	complement component factor h (Cfh)	5.27
Pddc1	Parkinson's disease 7 domain containing 1	4.56
Tgtp2	T cell specific GTPase 2	4.25
Lum	lumican	3.96
Hdac9	histone deacetylase 9 (Hdac9), transcript variant 2	3.88
Capn6	calpain 6	3.84
ENSMUST00000099684	Unknown	3.73
ENSMUST00000099050	Unknown	3.52
Fosb	FBJ osteosarcoma oncogene B	3.48
H2-K1	histocompatibility 2, K1, K region, transcript variant 1	3.44
Spp1	secreted phosphoprotein 1, transcript variant 5	3.36
ENSMUST00000099042	Unknown	3.34
Ear2	eosinophil-associated, ribonuclease A family, member 2	3.27
A_55_P1987086	Unknown	3.25
Mt2	metallothionein 2	-4.78
Thbd	thrombomodulin	-4.89
Trnp1	TMF1-regulated nuclear protein 1	−5.21
Hspb1	heat shock protein 1	-5.23
Smpdl3a	sphingomyelin phosphodiesterase, acid-like 3A	-5.26
Mest	mesoderm specific transcript, transcript variant 1	-5.28
Hs6st2	heparan sulfate 6-O-sulfotransferase 2	-5.34
Gm5493	9 days embryo whole body cDNA, RIKEN full-length enriched library, clone: D030063M22 product: weakly similar to Hypothetical KRAB box containing protein	-5.41
Mgmt	O − 6-methylguanine-DNA methyltransferase	-5.53
Slit3	slit homolog 3 (*Drosophila*)	-5.90
Gas6	growth arrest specific 6	−6.20
Pcp4	Purkinje cell protein 4	−6.53
Mest	mesoderm specific transcript, transcript variant 2	-6.94
Slc17a3	solute carrier family 17 (sodium phosphate), member 3	−7.66
Rspo3	R-spondin 3 homolog (*Xenopus laevis*)	−8.13

hydrolyze nucleoside diphosphates and triphosphates, which may play a role in purinergic signalling (Gorelik et al., 2016).

TMF-1 regulated nuclear protein 1 (TRNP1), coded by *Trnp1* gene, is a basic protein which accumulates in an insoluble nuclear fraction in mammalian cells, that can accelerate cell cycle progression (Volpe et al., 2006).

Another down-regulated gene in cells from F1 *focus* is *Thbd*, coding for thrombomodulin (TM), a protease with a role in TM dependent protein C activation, essential for mitochondrial function and myelination in CNS (Wolter et al., 2016). Loss of TM-dependent PC generation impairs primarily mitochondrial function and not mitochondrial biogenesis, suggesting a protective role for TM in CNS against oxidative stress.

Two more genes, *Mt2* and *Hspb1* coding for metallothionein 2 and heat shock protein 1 respectively, are down-regulated in cells from F1 *focus*.

3.2. Differentially expressed genes (DEGs) in F2 focus

Table 2 lists the top 15 up-regulated and down-regulated genes in cells from F2 *focus*. Among the most up-regulated genes, we found *Efemp1*, coding for the glycoprotein fibulin-3, which is normally expressed along the primary olfactory pathway and produced by olfactory epithelium cells *in vitro* (Vukovic et al., 2009). Fibulin-3 belongs to a small family of glycoproteins that normally have widespread distribution in extracellular matrix structures such as basement membranes, microfibrils and elastic fibres (Argraves et al., 1990; Timpl et al., 2003; de Vega et al., 2009). Based on its interaction with the tissue inhibitor of metalloproteinases-3 (TIMP-3) (Klenotic et al., 2004), a critical role for fibulin-3 in regulating matrix metalloproteinase (MMP) activity has been proposed (McLaughlin et al., 2007). Manipulation of fibulin-3 expression in cultured olfactory epithelium cells has been shown to alter both proliferation and migration (Vukovic et al., 2009).

Ras-activating protein-like 3 (RASAL3), encoded by *Rasal3* up-regulated gene, is a T cell-specific Ras GTPase-activating protein, that negatively regulates T cell receptor (TCR)-induced activation of Ras/MAPK pathway. Collectively, RASAL3 controls the magnitude of inflammatory responses through the survival of both naive T cells and activated T cells *in vivo* (Muro et al., 2018).

Follistatin-like 4, a SPARC-related protein-containing immunoglobulin domains 1 (SPIG1) encoded by *Fstl4* gene, was identified as one of the dorsal-retina-specific molecules expressed in the developing chick retina. SPIG1 negatively regulates Brain Derived Neurotrophic Factor maturation, thereby suppressing axonal branching and spine formation (Suzuki et al., 2014).

Other up-regulated genes in cells from F2 *focus* are *Chat*, coding for choline acetyltransferase, *Xlr3b*, coding for X-linked lymphocyte-regulated 3B, and *Resp18*, coding for Regulated endocrine-specific protein,18 kDa; the latter is a unique endoplasmic reticulum resident protein with an unknown function, first identified as a dopaminergic drugs-regulated intermediate pituitary transcript.

Also related to immunological signalling is *Ccl2* gene, coding for chemokine (C−C motif) ligand 2 (previously named MCP-1), one of the most important members of the CC chemokines family, involved in the regulation of oriented migration and the infiltration of mainly reticuloendothelial system cells, specifically monocyte/macrophage phenotypes. Fundamental roles are played by CCL2 and its related receptor (the CCR2) in brain tumours and in migration of monocytes from the bloodstream through the vascular endothelium (Vakilian et al., 2017). CCL2 is a potent monocyte-attracting chemokine and greatly contributes to the recruitment of blood monocytes into sites of inflammatory responses and tumours. Although tumour cells are considered to be the main source of CCL2, various non-tumour cells in the tumour stroma also produce CCl2 in response to stimuli.

Spp1 gene coding for Osteopontin is up-regulated also in cells from F2 *focus*. The last up-regulated gene with a known function, *Olfml2a*, codes for olfactomedin-like 2A, belonging to the OLF (olfactomedin)-family, a major component of the extracellular mucus matrix of olfactory neuroepithelium (Furutani et al., 2005).

Table 2
List of top 15 up- and down-regulated genes in cells from F2 *focus*. DEGs are listed in descending order of fold change compared to TPA-treated cell clone.

GeneName	Description	Fold change
Efemp1	epidermal growth factor-containing fibulin-like extracellular matrix protein 1	4.1
Rasal3	RAS protein activator like 3	4.04
Fstl4	follistatin-like 4	3.97
ENSMUST00000188511	tc|Q5SR98_MOUSE (Q5SR98) Ortholog of human Ras association (RalGDS\/AF-6) and pleckstrin homology domains 1 RAPH1 (Fragment), complete [TC1598183]	3.86
chr14:26093652–26,208,156_R	lincRNA: chr14:26093652–26,208,156 reverse strand	3.61
Chat	choline acetyltransferase	3.51
chr18:63480341–63,480,899_R	lincRNA: chr18:63480341–63,480,899 reverse strand	3.51
D6Ertd527e	DNA segment, Chr 6, ERATO Doi 527, expressed, transcript variant 1	3.45
ENSMUST00000181143	RIKEN cDNA B230104I21 gene (B230104I21Rik), misc_RNA	3.25
Xlr3b	X-linked lymphocyte-regulated 3B	3.24
Resp18	regulated endocrine-specific protein 18	3.14
Ccl2	chemokine (C−C motif) ligand 2	3.08
Spp1	secreted phosphoprotein 1, transcript variant 5	2.97
Olfml2a	olfactomedin-like 2A	2.96
chr2:150496011–150,496,503_R	lincRNA: chr2:150496011–150,496,503 reverse strand	2.93
2610008E11Rik	RIKEN cDNA 2610008E11 gene	−3.97
Hyi	hydroxypyruvate isomerase homolog (*E. coli*), transcript variant 1	−3.98
Gstt3	glutathione S-transferase, theta 3	−4.14
Olfr464	olfactory receptor 464	−4.30
Mest	mesoderm specific transcript, transcript variant 1	−4.71
Fbln7	fibulin 7	−4.75
Scrn1	secernin 1	−4.88
Hspb1	heat shock protein 1	−4.96
Gm5493	9 days embryo whole body cDNA, RIKEN full-length enriched library, clone: D030063M22 product: weakly similar to Hypothetical KRAB box containing protein (Fragment) [*Mus musculus*], full insert sequence	−5.12
Mgmt	O-6-methylguanine-DNA methyltransferase	−5.21
Thbd	thrombomodulin	−5.35
Rspo3	R-spondin 3 homolog (*Xenopus laevis*) (Rspo3),	−5.37
ENSMUST00000019268	mRNA for mKIAA0193 protein	−5.63
Mest	mesoderm specific transcript, transcript variant 2	−6.06
Slc17a3	solute carrier family 17 (sodium phosphate), member 3, transcript variant 1	−7.88

Among the top 15 down-regulated genes in cells from F2 *focus* we found many genes which are also down-regulated in F1 *focus*, such as *Slc17a3*, *Mest*, *Rspo3*, *Thbd*, *Mgmt*, *Hspb1*, as well as *Gm5493* gene, whose product is unknown.

Among the genes exclusively up-regulated in F2 *focus* we found *Scrn1*, coding for Secernin 1, a brain cytosolic protein, with a putative dipeptidase activity, also capable of regulating exocytosis in permeabilized mast cells (Way et al., 2002), and *Fbln7*, coding for fibulin-7 (FBLN7), also called TM14, a cell adhesion molecule that interacts with extracellular matrix molecules in teeth (de Vega et al., 2007). Argraves and coworkers (Argraves et al., 1990) described the first member of this family, fibulin-1, as a binding partner for the fibronectin receptor integrin and an important regulator of cell adhesion. So far, 5 other members (fibulins 2–6) have been identified, modulating cell morphology, growth, adhesion, and motility. In addition, it has been demonstrated that the dysregulation of some fibulins is linked to cancer, and both tumour suppressive and pro-oncogenic roles have been proposed for members of the fibulin family (Gallagher et al., 2005).

3.3. Differentially expressed genes (DEGs) in F3 focus

As shown in Table 3, among the 15 top up-regulated genes in F3 *focus*, we found a series of genes coding for 2′-5′ oligoadenylate synthetases (OAS), such as *Oas1a*, *Oas1f*, *Oas2* and *Oasl2*. OAS proteins are interferon (IFN) inducible pathogen recognition receptors expressed in different cell types. Upon activation by the pathogen-associated molecular pattern (PAMP) double-stranded viral RNA, certain OAS proteins synthesize 2′-5′- oligoadenylate (2-5A), which activates RNase L (Silverman and Weiss, 2014). In mice, there are 8 *Oas1* genes (Mashimo et al., 2003; Perelygin et al., 2006; Kristiansen et al., 2011); however, only *mOAS1a* and *mOAS1g* are believed to be enzymatically active. Mice have four additional *Oas* genes, which produce 3 enzymatically active proteins (mOAS2, mOAS3 and mOASL2), and one inactive (mOASL1) protein (Kakuta et al., 2002).

With two exceptions, namely *Usp18* and *Rtp4*, all other genes up-regulated in cells from F3 *focus* code for proteins involved in IFN mediated antiviral response: *Ifi44*, coding for interferon-induced protein 44; *Sp110*, coding for Sp110 nuclear body protein, an interferon induced transcriptional coactivator with a bound zinc atom highly expressed in leukocytes; *Mx1*, coding for myxovirus resistance 1 protein; *Isg15*, coding for ISG15 ubiquitin-like modifier; H2-K1, histocompatibility K region; *Ifi27l2a*, coding for interferon alpha-inducible protein27 like 2A, and *Tgtp2*, coding for T cell specific GTPase 2. Ifi2712a belongs to a family of small interferon induced hydrophobic proteins, the ISG12 proteins; the expression of *ISG12b1*, also called *IFI27*, has been reported to be up-regulated in the mouse brain after intracerebral virus infection. Moreover, *ISG12b1* has been identified as an adipose-specific gene, localized in mitochondria: current studies demonstrate that its overexpression in 3 T3-L1 cells inhibits mitochondrial biogenesis and lipid accumulation in adipocytes (Li et al., 2009).

Usp18 codes for ubiquitin-specific protease 18, a deubiquitinating enzyme (DUB) catalysing the deconjugation of ubiquitin chains from ubiquitinated proteins (Komander et al., 2009). Many studies have demonstrated that some DUBs are the signalling targets of cellular stress such as oxidative stress. In mouse, *Usp18* was found to be induced by oxidative stress, in a dose- and time-dependent manner, while its depletion could stimulate an increase in p53 and caspase 3 protein levels. This suggests that *Usp18* protects the cells from oxidative stress-induced apoptosis, likely through the regulation of p53 and caspase 3 (Lai et al., 2017). DUBs can regulate p53 signalling pathway *via* different mechanisms within different cellular compartments in response to different kinds of stresses (Kwon et al., 2017).

Rtp4 codes for receptor transporter protein 4, a member of the RTP protein family specifically expressed in olfactory neurons. These proteins are normally associated with olfactory receptors (OR) proteins and enhance OR responses to odorants (Saito et al., 2004).

Table 3
List of top 15 up- and down-regulated genes in cells from F3 *focus*. DEGs are listed in descending order of fold change compared to TPA-treated cell clone.

GeneName	Description	Fold change
Oas1a	2′-5′ oligoadenylate synthetase 1A	7.68
Oas1f	2′-5′ oligoadenylate synthetase 1F	6.31
Oas2	2′-5′ oligoadenylate synthetase 2	6.09
Ifi44	interferon-induced protein 44	5.58
Gm9706	predicted gene 9706	5.54
Sp110	Sp110 nuclear body protein	5.48
Mx1	myxovirus (influenza virus) resistance 1	5.39
Oasl2	2′-5′ oligoadenylate synthetase-like 2	5.38
Isg15	ISG15 ubiquitin-like modifier	5.30
H2-K1	histocompatibility 2, K1, K region	5.30
LOC100041034	Sp110 nuclear body protein-like	5.30
Ifi27l2a	interferon, alpha-inducible protein 27 like 2A	5.24
Tgtp2	T cell specific GTPase 2	5.19
Usp18	ubiquitin specific peptidase 18	4.97
Rtp4	receptor transporter protein 4	4.90
Papss2	3′-phosphoadenosine 5′-phosphosulfate synthase 2	−3.20
Mest	mesoderm specific transcript	−3.21
Ppp1r1b	protein phosphatase 1, regulatory (inhibitor) subunit 1B	−3.23
Rpe65	retinal pigment epithelium 65	−3.28
Col11a1	collagen, type XI, alpha 1	−3.37
Speer2	spermatogenesis associated glutamate (*E*)-rich protein 2	−3.42
1190002H23Rik	RIKEN cDNA 1190002H23 gene	−3.47
Sorl1	sortilin-related receptor, LDLR class A repeats-containing	−3.65
4933402N22Rik	RIKEN cDNA 4,933,402 N22 gene	−3.67
Arxes2	adipocyte-related X-chromosome expressed sequence 2	−3.72
Plxdc2	plexin domain containing 2	−3.82
Pcp4	Purkinje cell protein 4	−4.01
Igf1	insulin-like growth factor 1	−4.54
Fos	FBJ osteosarcoma oncogene	−4.56
Col2a1	collagen, type II, alpha 1	−6.72

Among the top 15 genes down-regulated in cells from F3 *focus*, also listed in Table 3, we found the *Mest* gene, which is found among the 15 top down-regulated genes of cells from F1 and F2 *foci*. Two genes coding for collagen, *Col2a1* and *Col11a1* are also down-regulated in this *focus*, as well as *Pcp4* gene, which is one of the most strongly down-regulated genes in F1 *focus*. Interestingly, *Fos* gene, promoting cell survival, was found to be down-regulated in F3 *focus*, while it is found among the most up-regulated genes in F1 *focus*. The same is true for *Igf1* gene, coding for insulin-like growth factor 1, which plays a key role in the development and progression of many human cancers. Moreover, a large amount of data supports that insulin-like growth factor 1 (IGF-1) deficiency increases insulin resistance, impairs lipid metabolism, promotes oxidative damage, and dysregulates the GH/IGF-1 axis (Gonzalez-Guerra et al., 2017).

Another down-regulated gene in cells from F3 *focus* is *Plxdc2* gene, coding for plexin domain containing 2. Direct molecular activity of Plxdc2 has been demonstrated in the control of proliferation, its expression being altered in various kinds of cancer; in particular, Plxdc2 has been shown to act as a mitogen in the developing nervous system (Miller-Delaney et al., 2011).

Arxes2 gene, coding for adipocyte-related X-chromosome expressed sequence 2, is required for fat cells differentiation and is transactivated by adipogenic transcription factors.

Sorl1 gene codes for sortilin-related receptor, an LDLR class A receptor with a cysteine-rich repeat that plays a central role in mammalian cholesterol metabolism, as well as in cell migration and metabolic regulation (Schmidt et al., 2016).

Speer2 gene codes for spermatogenesis associated glutamate (*E*)-rich protein 2, a new group of haploid sperm-specific nuclear factors (Spiess et al., 2003).

RPE65, the product of *Rpe65* gene, is an enzyme involved in vitamin A metabolism in retinal pigment epithelium (RPE) cells (Redmond et al., 1998), where it is necessary for production of 11-cisvitamin A in the retinal visual cycle. Mutations in *Rpe65* are associated with several retinal disorders. Pyakurel and coworkers demonstrated that the disruption of ERK1/2 specifically in RPE cells leads to a marked decrease of RPE65 expression, while the activation of ERK1/2 is associated with the activation of the Wnt/β-catenin pathway, which plays a key role in the expression of the RPE-specific transcription factors (Pyakurel et al., 2017).

Two more genes were found down-regulated in cells from F3 *focus*: *Papss2*, coding for 3′-phosphoadenosine 5′-phosphosulfate synthase 2, and *Ppp1r1b* encoding protein phosphatase, inhibitor subunit 1b, a bifunctional signal transduction molecule.

3.4. Cytokines encoding genes are up-regulated in cells from all foci

The Venn Diagram in Fig. 1A shows the number of the differentially expressed genes (DEGs) in the cells from the three *foci*. On the whole, cells from F3 *focus* undergo the highest gene expression deregulation, with 1091 DEGs, while cells from F2 seem to be the less changed by Cd treatment, with only 126 DEGs; the cells from F1 *focus* present an intermediate situation with 255 DEGs. Only 34 genes are deregulated in all three *foci*, although not to the same extent, and are all listed in Table 4 and graphically represented in Fig. 1B. Table 4 shows that the only genes up-regulated in all three *foci* are genes coding for cytokines: *Ccl2*, *Ccl5*, *Il6* and *Spp1*. Among the 34 DEGs common in all *foci*, the majority (23) appears to be down-regulated in all *foci*, while only 4 are down-regulated in both F1 and F2 *foci* and up-regulated in F3 *focus*; only one gene (*Marcksl1*, coding for MARCKS-like 1 protein) is up-regulated in both F1 and F2 *foci* and down-regulated in F3 *focus*, while *Thy1* gene, coding for thymus cell antigen 1, is down-regulated in F1 *focus* and up-regulated in both F2 and F3 *foci*.

The validation through RT-PCR confirmed *Il-6* gene up-regulation in all three *foci*. The relative quantification of Interleukin-6 mRNA was carried out through real-time quantitative PCR in cells from all three *foci*, using *β*-actin as internal reference control, and TPA-treated cells as a calibrator. The results, reported in Fig. 2, showed *Il-6* gene to be up-regulated in all three *foci*, with a higher fold change in F1 *focus*, compared to both F2 and F3 *foci*.

3.5. Gene Ontology enrichment analysis

The DEGs detected in microarrays from the three *foci* were subjected to a Gene Ontology (GO) enrichment analysis, as described in Materials and Methods. Results reported in Fig. 3 show the presence, in all *foci,* of dysregulated gene expression in the “angiogenesis” category, which includes some up-regulated genes, like *Spp1*, coding for osteopontin, or down-regulated genes, like *Mest* and *Plxdc2*. Other categories showing dysregulated genes in all *foci* concern organ and tissue morphogenesis, as well as extracellular organization; however, none of these categories is common to all *foci*. Dysregulated genes in “extracellular structure organization” are found in F2 and F3 *foci* (Fig. 3B and 3C), but not in F1 (Fig. 3A). However, F1 *focus* shows dysregulated genes in connective tissue, muscle organ and skeletal system development, as well as in “regulation of animal morphogenesis”, “extracellular organization” and “tissue morphogenesis” (Fig. 3A). Moreover, only F1 *focus* shows dysregulation of genes related to negative regulation of growth, a category including many growth factors, as well as different chemokines and interleukins, leading to a loss of growth regulation.

Apart from genes involved in regulation of cell morphogenesis, skeletal system development and extracellular structure organization, most of dysregulated genes in F3 *focus* belong to categories related to immune defence, like “regulation of innate immunity response”, “response to virus”, “positive regulation of defence response”, “response to beta and gamma interferons” (Fig. 3C).

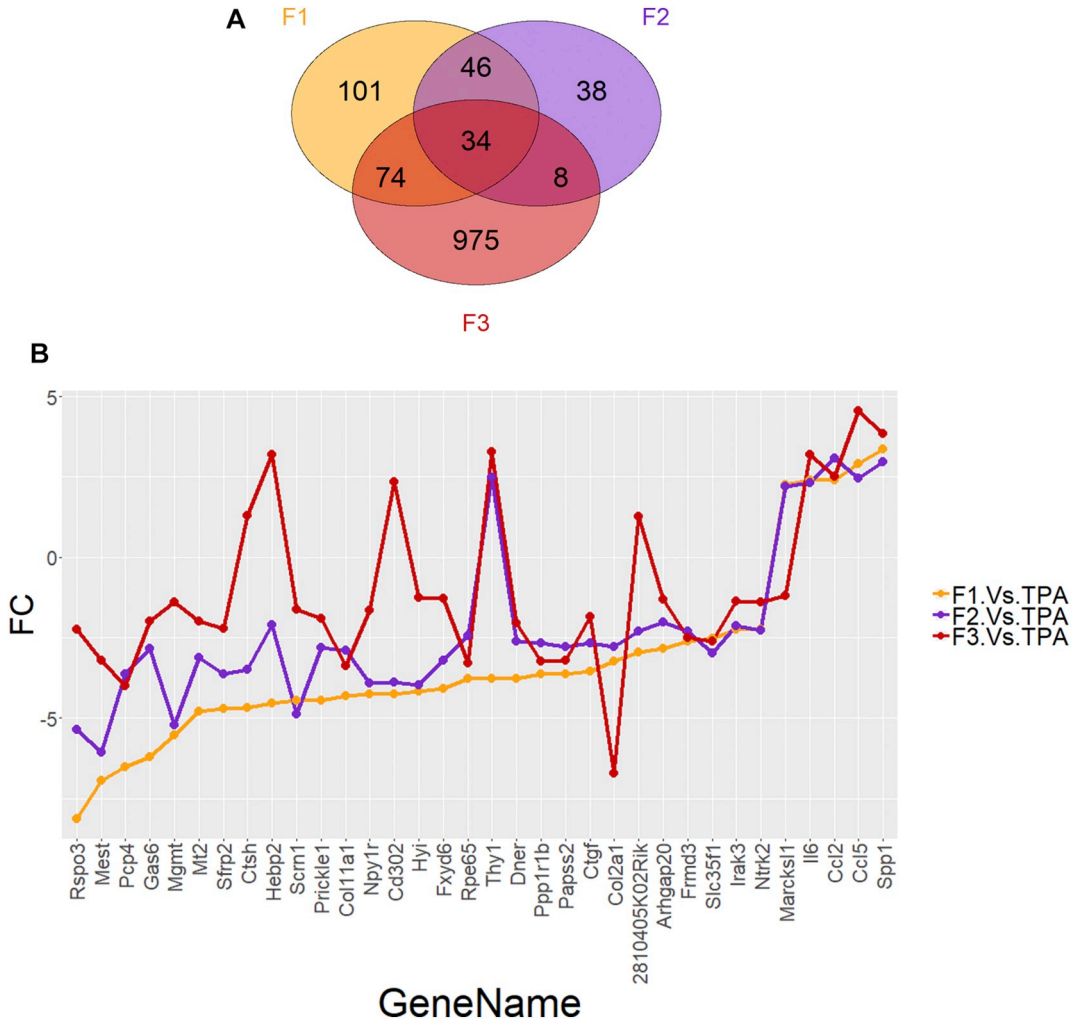

Fig. 1. Differentially expressed genes (DEGs) in the three different *foci* (F1, F2, and F3) analyzed: A) Venn Diagram of DEGs (both up and down) for the three *foci*; B) Plot of fold change (FC) on y-axis of the genes differentially expressed in all the three *foci* (see Table 4). Colours represent the three different *foci*. Genes are ordered by the comparison F1 *vs* TPA.

As shown in Fig. 3B, some dysregulated genes related to immune response are also found in F2 *focus* in the "chemiotaxis" category, including chemokines coding genes, as well as *Gas6* and *Fgf4* genes.

4. DISCUSSION

Comparing the lists of differentially expressed genes (DEGs) in the cells from the three *foci*, it is evident that a common stimulus (1μM $CdCl_2$ for 24h) administered to the healthy C3H10T1/2 cells elicits different cellular responses, as preliminarily shown by our group (Forcella et al., 2016). Most of the cells treated with $CdCl_2$ have efficient defence mechanisms, demonstrated by the up-regulation of metallothioneins and Hsp70 in the first hours after cadmium administration, followed by their down-regulation (Callegaro et al., 2018). However, a few cells, cannot efficiently counteract the insult and develop different metabolic alterations (Forcella et al., 2016), leading to cell transformation and *foci* formation in the weeks following cadmium treatment.

DEGs analysis, performed in this work, confirms these differences, showing only 34 common DEGs in cells from the different *foci*; among these, only 4 genes are up-regulated in all *foci*: *Ccl2*, *Ccl5*, *IL6* and *Spp1*, all coding for chemokines. Although chemokines were first discovered as mediators of migration of immune cells to sites of inflammation and injury, they are now known to play multiple roles in organ development, angiogenesis, and tumorigenesis. In particular, recent data show that CCl2 production regulates the interactions between tumour cells and macrophages, promoting tumour progression (Yoshimura, 2018).

Gene Ontology (GO) enrichment analysis, performed on all DEGs in the three *foci,* shows that inflammation, and therefore cytokines production, is involved in many of the identified pathways, like "cell chemiotaxis", "positive regulation of defence response", "response to viruses" and "regulation of immune innate response". The up-regulation of inflammatory pathways is less evident in F1 *focus*, where genes connected with up-regulation of cell growth and extracellular matrix rearrangement prevail, in accordance with its highly proliferative behaviour; this confirms data from a previous work by our group (Forcella et al., 2016), showing that, while the ERK proliferative pathway is activated in F1 *focus*, the survival pathway mediated by Akt is activated in F3 *focus*. The down-regulation of both *Fosb* and *Igf1* genes in F3 *focus*, as well as the up-regulation of *Fosb* gene in F1 *focus*, likely accounts for this difference in proliferation.

On the other hand, we found that most common DEGs are down-regulated; among these, are genes coding for proteins of the extracellular matrix, like *Mest*, *Col11a1*, *Col2a1* and *Ctgf*, and genes coding for proteins involved in cell growth arrest, such as *Gas6*, *Rspo3* and *Mgmt*. suggesting major rearrangements of the extracellular matrix leading to cell cycle progression. A major rearrangement of extracellular matrix is confirmed also by GO analyses, showing "regulation of animal morphogenesis", "connective tissue development", as well as "regulation of cell morphogenesis" and "extracellular structural

Table 4
Differentially expressed genes in all cell clones from F1, F2, and F3 *foci*.

Gene name	Description	Fold change		
		F1	F2	F3
2810405K02Rik	RIKEN cDNA 2,810,405 K02 gene	−2.94	−2.31	1.27
Arhgap20	Rho GTPase activating protein 20	−2.85	−2.02	−1.32
Ccl2	chemokine (C−C motif) ligand 2	2.41	3.08	2.50
Ccl5	chemokine (C−C motif) ligand 5	2.92	2.45	4.54
Cd302	CD302 antigen	−4.24	−3.89	2.33
Col11a1	collagen, type XI, alpha 1	−4.32	−2.90	−3.37
Col2a1	collagen, type II, alpha 1	−3.24	−2.77	−6.72
Ctgf	connective tissue growth factor	−3.55	−2.66	−1.85
Ctsh	cathepsin H	−4.69	−3.48	1.30
Dner	delta/notch-like EGF-related receptor	−3.76	−2.60	−2.05
Frmd3	FERM domain containing 3	−2.60	−2.31	−2.50
Fxyd6	FXYD domain-containing ion transport regulator 6	−4.07	−3.21	−1.27
Gas6	growth arrest specific 6	−6.20	−2.85	−1.98
Hebp2	heme binding protein 2	−4.54	−2.11	3.18
Hyi	hydroxypyruvate isomerase homolog (*E. coli*)	−4.17	−3.98	−1.26
Il6	interleukin 6	2.39	2.32	3.18
Irak3	interleukin-1 receptor-associated kinase 3	−2.25	−2.13	−1.37
Marcksl1	MARCKS-like 1	2.27	2.19	−1.19
Mest	mesoderm specific transcript	−6.94	−6.06	−3.21
Mgmt	O-6-methylguanine-DNA methyltransferase	−5.53	−5.21	−1.40
Mt2	metallothionein 2	−4.78	−3.12	−1.99
Npy1r	neuropeptide Y receptor Y1	−4.26	−3.92	−1.65
Ntrk2	neurotrophic tyrosine kinase, receptor, type 2	−2.25	−2.27	−1.40
Papss2	3'-phosphoadenosine 5'-phosphosulfate synthase 2	−3.62	−2.79	−3.20
Pcp4	Purkinje cell protein 4	−6.53	−3.63	−4.01
Ppp1r1b	protein phosphatase 1, regulatory (inhibitor) subunit 1B	−3.64	−2.68	−3.23
Prickle1	prickle homolog 1 (*Drosophila*)	−4.46	−2.80	−1.89
Rpe65	retinal pigment epithelium 65	−3.78	−2.45	−3.28
Rspo3	R-spondin 3 homolog (*Xenopus laevis*)	−8.13	−5.37	−2.23
Scrn1	secernin 1	−4.46	−4.88	−1.61
Sfrp2	secreted frizzled-related protein 2	−4.72	−3.64	−2.21
Slc35f1	solute carrier family 35, member F1	−2.54	−2.98	−2.60
Spp1	secreted phosphoprotein 1	3.36	2.97	3.83
Thy1	thymus cell antigen 1, theta	−3.78	2.48	3.28

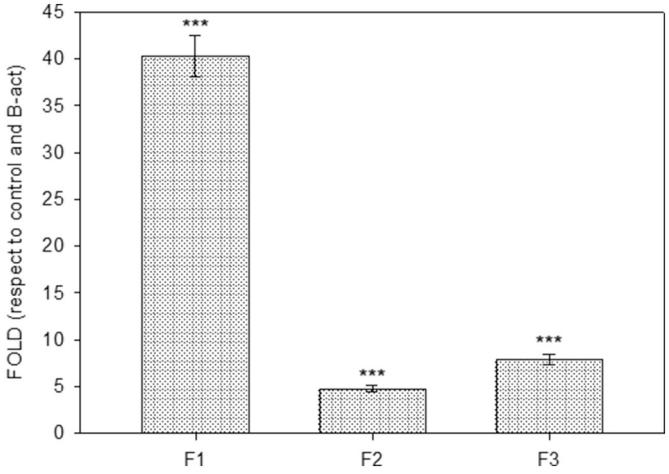

Fig. 2. Relative quantification of Interleukin-6 mRNA levels by real-time quantitative PCR in F1, F2, F3 cell clones.
The relative expression level was calculated with the Livak method ($2[-\Delta\Delta C(T)]$) and was expressed as a fold change ± SD, using β-actin gene as internal reference control and the TPA-treated cell clone as calibrator. *** $P < 0.001$ (Dunnett's test).

organization" among the most deregulated pathways.

On the whole gene expression dysregulation induced by $CdCl_2$ seems to be achieved more through gene down-regulation than up-regulation: in F1 *focus*, apart from the most up-regulated gene (showing a fold change higher than 12), the other top up-regulated genes show an average fold of 4, in contrast with the top down-regulated genes, all showing folds higher than 5. The same is true for F2 *focus*, although with smaller overall fold values, showing higher values for top down-regulated genes than for up-regulated ones. In contrast, in F3 *focus*, the top 15 up- and down-regulated genes show similar fold values.

F1 and F2 *foci* are more similar to each other than to F3 *focus*, showing 8 identical top down-regulated genes out of 15. An intriguing feature of F2 *focus* is the down-regulation of two genes coding for olfactory receptors (OR); many other OR encoding genes were previously found to be down-regulated upon 24 hours treatment with cadmium (Callegaro et al., 2018). Although the meaning of this down-regulation is not clear, about 1500 genes coding for olfactory receptors are present in mouse genome and these receptors are also expressed in a variety of non-olfactory tissues (Zhang et al., 2016; Ichimura et al., 2008; Pluznick et al., 2013). Moreover, several predicted mammalian OR genes are solely expressed in non-olfactory tissues, raising the possibility that the receptors have functions other than odour recognition. Although still debated, OR are probably either Zn or Cu binding proteins, their dysregulation being due to Zn/metals homeostasis disruption.

Although significant differences are observed when comparing F1 and F2 top up-regulated genes, the only common DEG being *Spp1*, on the whole, the same pattern of cell matrix rearrangement and inflammatory response up-regulation emerges in cells from both *foci*, involving genes such as *Mest*, *Lum*, *Slit3* and *Hs6st2*, *Efemp1*, *Fbln7*, coding for cell matrix proteins, and *Spp1*, *Cfh*, *Tgtp2*, *Rasal3*, *Resp18*, *Ccl2* and *Xlr3b*, involved in inflammation. Moreover, many proteins encoded by DEGs have been previously reported to be oncogenic, like *Fosb, Hdac9* and *Gas6,* dysregulated in F1 *focus*, and *Mgmt, Rspo3* and *Thbd,* dysregulated in both F1 and F2 *foci*.

A completely different picture emerges from the top up- and down-regulated genes in F3 *focus*; in particular, 13 out of the 15 top up-regulated genes are involved in an interferon mediated antiviral response, which can be triggered by either viral DNA or viral RNA. Efficient elimination of viral infection relies on both detection of the virus by pattern recognition receptors (PRRs) and inhibition of viral replication by antiviral restriction factors. Retinoic acid-inducible gene-I (*RIG-I*) is a PRR that upon activation by primarily 5'-triphosphate RNA induces a signalling cascade leading to interferon (IFN) gene expression.

The 2'-5' oligoadenylate synthetases (OASs) are a family of IFN- and virus-induced antiviral restriction factors that provide protection against a wide spectrum of RNA and DNA viruses. Initial virus detection induces the expression of OASL, which, upon subsequent virus detection, can promote RIG-I signalling thereby enhancing the antiviral response (Ibsen et al., 2015). However, a similar response has been shown to be triggered also by mitochondrial damage releasing mtDNA into the cytosol. *Thbd* gene down-regulation in both F1 and F2 *foci* also suggests mitochondrial damage, loss of Thrombomodulin-dependent PC activation impairing mitochondrial functionality. GO enrichment analysis confirms the strong up-regulation of inflammatory response in F3 *focus*, showing pathways like "response to viruses", "positive regulation of defence response", "regulation of immune innate response" and "response to interferon gamma" are among the most dysregulated.

5. Conclusions

Our previous work on up- and down-regulated genes and functions, immediately after 24 hours exposure to 1 μM $CdCl_2$ and after a period of recovery, showed that the cells respond mainly by activating defence mechanisms, that decrease in the following recovery period. These

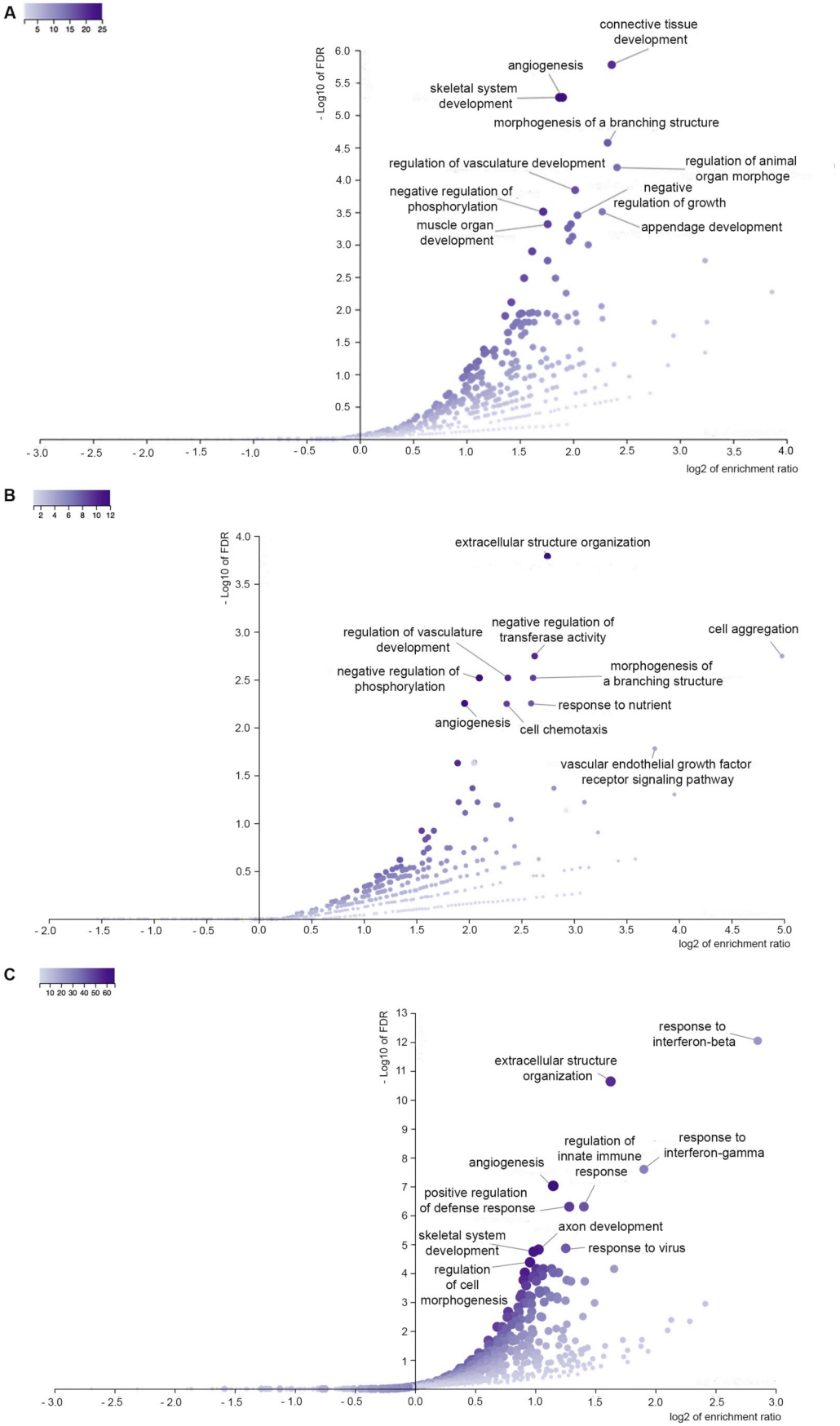

Fig. 3. Functional enrichment analysis

Each volcano plot shows the log of False Discovery Rates (FDR) against enrichment ratio for all the Gene Ontology categories. The gene set name showed in the volcano plot are representative of the TOP 10 categories based on the FDR. For example, the most significant categories are shown in the upper part of the plots. The size and colour of the dots are proportional to the size of the category. Volcano plots represent the Enrichment results of F1 (A), of F2 (B), and of F3 cell clones (C).

defence mechanisms are generally very efficient, however a few cells evade them and proliferate or survive in an uncontrolled manner (Forcella et al., 2016; Callegaro et al., 2018). This leads to the formation of *foci* derived from different transformed cell clones. The features of deregulated genes in each *focus,* analyzed in this work, suggest that different functional targets (proteins and/or processes) are involved in the complex mechanism of cell transformation. However, it is noteworthy that the only genes in common to all analyzed *foci* are those responsible for cytokine/chemokines coding. These genes are involved in the inflammatory response, which is a known feature of carcinogenesis (see for example (Coussens and Werb, 2002; Suarez-Carmona et al., 2017). In addition, in F3 *focus* the inflammatory response is likely related to mitochondrial damage.

Thus, it appears that the significant signal triggering the process of Cd-induced transformation in C3H cells could be mainly represented by the deregulation of zinc homeostasis. The interference of Cd on Zn homeostasis has previously been demonstrated by our group and is also described in the literature (Callegaro et al., 2018; Urani et al., 2015; Martelli et al., 2006). Moreover, our present work stresses the relevance of the cell transformation assays (CTAs) not only as *in vitro* methods for the evaluation of the carcinogenesis potential of chemicals, but also as powerful tools for the comprehension of the mechanisms underlying the process of cell transformation.

The *in vitro* and bioinformatics mechanistic-based approach of this work, along with novel integrated *in vitro* carcinogenicity test on multiple cellular endpoints (Wilde et al., 2018) is in agreement with the just published suggestions (Madia et al., 2019) on performing *ad hoc* studies sorted on the basis of cancer's hallmarks, and organised in the form of Integrated Approaches to Testing and Assessment (IATA). This would provide a better understanding of cancer induction by environmental contaminants, also in view of its prevention, and could progress the exploit of *in vitro* carcinogenicity evaluation.

Further, although our work is preliminary and additional studies will be necessary, the identification of specific structures/processes deregulated in transformed cells could represent an important starting point for the development of anti-tumour agents targeting specific cell functions in transformed cells. In this context, the use of CTAs represents an invaluable means to perform preliminary studies in a controlled and relatively simple environment, in comparison to the *in vivo* situation.

Declaration of Competing Interest

The authors declare that they have no known competing financial interests or personal relationships that could have appeared to influence the work reported in this paper.

Acknowledgements

The authors acknowledge the European Commission. CU acknowledges the partial support by Fondo di Ateneo (University of Milano - Bicocca, 2016-ATE-0411); PF acknowledges the partial support by Fondo di Ateneo (University of Milano - Bicocca, 2017-ATE-0273). The authors acknowledge Gerard Bowe for manuscript revisions.

References

Aerts, J., Laeremans, A., Minerva, L., Boonen, K., Harshavardhan, B., D'Hooge, R., Valkenborg, D., Baggerman, G., Arckens, L., 2017. MS imaging and mass spectrometric synaptosome profiling identify PEP-19/pcp4 as a synaptic molecule involved in spatial learning in mice. Biochim Biophys Acta Proteins Proteom 1865, 936–945. https://doi.org/10.1016/j.bbapap.2016.10.007.

Ao, L., Liu, J.Y., Liu, W.B., Gao, L.H., Hu, R., Fang, Z.J., Zhen, Z.X., Huang, M.H., Yang, M.S., Cao, J., 2010. Comparison of gene expression profiles in BALB/c 3T3 transformed foci exposed to tumor promoting agents. Toxicol In Vitro 24, 430–438. https://doi.org/10.1016/j.tiv.2009.10.006.

Argraves, W.S., Tran, H., Burgess, W.H., Dickerson, K., 1990. Fibulin is an extracellular matrix and plasma glycoprotein with repeated domain structure. J Cell Biol 111, 3155–3164.

Callegaro, G., Forcella, M., Melchioretto, P., Frattini, A., Gribaldo, L., Fusi, P., Fabbri, M., Urani, C., 2018. Toxicogenomics applied to in vitro Cell Transformation Assay reveals mechanisms of early response to cadmium. Toxicol In Vitro 48, 232–243. https://doi.org/10.1016/j.tiv.2018.01.025.

Carlow, D.A., Teh, S.J., Teh, H.S., 1998. Specific antiviral activity demonstrated by TGTP, a member of a new family of interferon-induced GTPases. J Immunol 161, 2348–2355.

Choong, G., Liu, Y., Templeton, D.M., 2014. Interplay of calcium and cadmium in mediating cadmium toxicity. Chem Biol Interact 211, 54–65. https://doi.org/10.1016/j.cbi.2014.01.007.

Corvi, R., Madia, F., 2017. In vitro genotoxicity testing-Can the performance be enhanced? Food Chem Toxicol 106, 600–608. https://doi.org/10.1016/j.fct.2016.08.024.

Corvi, R., Madia, F., Guyton, K.Z., Kasper, P., Rudel, R., Colacci, A., Kleinjans, J., Jennings, P., 2017. Moving forward in carcinogenicity assessment: Report of an EURL ECVAM/ESTIV workshop. Toxicol In Vitro 45, 278–286. https://doi.org/10.1016/j.tiv.2017.09.010.

Coussens, L.M., Werb, Z., 2002. Inflammation and cancer. Nature 420, 860–867. https://doi.org/10.1038/nature01322.

Dear, N., Matena, K., Vingron, M., Boehm, T., 1997. A new subfamily of vertebrate calpains lacking a calmodulin-like domain: implications for calpain regulation and evolution. Genomics 45, 175–184. https://doi.org/10.1006/geno.1997.4870.

Fischer, M.M., Yeung, V.P., Cattaruzza, F., Hussein, R., Yen, W.C., Murriel, C., Evans, J.W., O'Young, G., Brunner, A.L., Wang, M., Cain, J., Cancilla, B., Kapoun, A., Hoey, T., 2017. RSPO3 antagonism inhibits growth and tumorigenicity in colorectal tumors harboring common Wnt pathway mutations. Sci Rep 7, 15270. https://doi.org/10.1038/s41598-017-15704-y.

Forcella, M., Callegaro, G., Melchioretto, P., Gribaldo, L., Frattini, M., Stefanini, F.M., Fusi, P., Urani, C., 2016. Cadmium-transformed cells in the in vitro cell transformation assay reveal different proliferative behaviours and activated pathways. Toxicol In Vitro 36, 71–80. https://doi.org/10.1016/j.tiv.2016.07.006.

Furutani, Y., Manabe, R., Tsutsui, K., Yamada, T., Sugimoto, N., Fukuda, S., Kawai, J., Sugiura, N., Kimata, K., Hayashizaki, Y., Sekiguchi, K., 2005. Identification and characterization of photomedins: novel olfactomedin-domain-containing proteins with chondroitin sulphate-E-binding activity. Biochem J 389, 675–684. https://doi.org/10.1042/BJ20050120.

Gallagher, W.M., Currid, C.A., Whelan, L.C., 2005. Fibulins and cancer: friend or foe? Trends Mol Med 11, 336–340. https://doi.org/10.1016/j.molmed.2005.06.001.

Gentleman, R.C., Carey, V.J., Bates, D.M., Bolstad, B., Dettling, M., Dudoit, S., Ellis, B., Gautier, L., Ge, Y., Gentry, J., Hornik, K., Hothorn, T., Huber, W., Iacus, S., Irizarry, R., Leisch, F., Li, C., Maechler, M., Rossini, A.J., Sawitzki, G., Smith, C., Smyth, G., Tierney, L., Yang, J.Y., Zhang, J., 2004. Bioconductor: open software development for computational biology and bioinformatics. Genome Biol 5, R80. https://doi.org/10.1186/gb-2004-5-10-r80.

Geutskens, S.B., Hordijk, P.L., van Hennik, P.B., 2010. The chemorepellent Slit3 promotes monocyte migration. J Immunol 185, 7691–7698. https://doi.org/10.4049/jimmunol.0903898.

Gonzalez-Guerra, J.L., Castilla-Cortazar, I., Aguirre, G.A., Munoz, U., Martin-Estal, I., Avila-Gallego, E., Granado, M., Puche, J.E., Garcia-Villalon, A.L., 2017. Partial IGF-1 deficiency is sufficient to reduce heart contractibility, angiotensin II sensibility, and alter gene expression of structural and functional cardiac proteins. PLoS One 12, e0181760. https://doi.org/10.1371/journal.pone.0181760.

Gorelik, A., Heinz, L.X., Illes, K., Superti-Furga, G., Nagar, B., 2016. Crystal Structure of the Acid Sphingomyelinase-like Phosphodiesterase SMPDL3B Provides Insights into Determinants of Substrate Specificity. J Biol Chem 291, 24054–24064. https://doi.org/10.1074/jbc.M116.755801.

Goudarzi, S., Rivera, A., Butt, A.M., Hafizi, S., 2016. Gas6 Promotes Oligodendrogenesis and Myelination in the Adult Central Nervous System and After Lysolecithin-Induced Demyelination. ASN Neuro 8. https://doi.org/10.1177/1759091416668430.

Habuchi, H., Kimata, K., 2010. Mice deficient in heparan sulfate 6-O-sulfotransferase-1. Prog Mol Biol Transl Sci 93, 79–111. https://doi.org/10.1016/S1877-1173(10)93005-6.

Hartwig, A, 2013. Cadmium and cancer. Met Ions Life Sci. 11, 491–507. https://doi.org/10.1007/978-94-007-5179-8_15.

Hilkens, J., Timmer, N.C., Boer, M., Ikink, G.J., Schewe, M., Sacchetti, A., Koppens, M.A.J., Song, J.Y., Bakker, E.R.M., 2017. RSPO3 expands intestinal stem cell and niche compartments and drives tumorigenesis. Gut 66, 1095–1105. https://doi.org/10.1136/gutjnl-2016-311606.

Hwang, S.H., Yeom, H., Eom, S.Y., Lee, Y.M., Lee, M., 2019. Genome-wide DNA methylation changes in transformed foci induced by non-genotoxic carcinogens. Environ Mol Mutagen. https://doi.org/10.1002/em.22285.

Ibsen, M.S., Gad, H.H., Andersen, L.L., Hornung, V., Julkunen, I., Sarkar, S.N., Hartmann, R., 2015. Structural and functional analysis reveals that human OASL binds dsRNA to enhance RIG-I signaling. Nucleic Acids Res 43, 5236–5248. https://doi.org/10.1093/nar/gkv389.

Ichimura, A., Kadowaki, T., Narukawa, K., Togiya, K., Hirasawa, A., Tsujimoto, G., 2008. In silico approach to identify the expression of the undiscovered molecules from microarray public database: identification of odorant receptors expressed in non-olfactory tissues. Naunyn Schmiedebergs Arch Pharmacol 377, 159–165. https://doi.org/10.1007/s00210-007-0255-6.

Jarup, L., Akesson, A., 2009. Current status of cadmium as an environmental health problem. Toxicol Appl Pharmacol 238, 201–208. https://doi.org/10.1016/j.taap.2009.04.020.

Jozsi, M., Schneider, A.E., Karpati, E., Sandor, N., 2018. Complement factor H family proteins in their non-canonical role as modulators of cellular functions. Semin Cell

Dev Biol. https://doi.org/10.1016/j.semcdb.2017.12.018.
Kakuta, S., Shibata, S., Iwakura, Y., 2002. Genomic structure of the mouse 2',5'-oligoadenylate synthetase gene family. J Interferon Cytokine Res 22, 981–993. https://doi.org/10.1089/10799900260286696.
Kaneko-Ishino, T., Kuroiwa, Y., Miyoshi, N., Kohda, T., Suzuki, R., Yokoyama, M., Viville, S., Barton, S.C., Ishino, F., Surani, M.A., 1995. Peg1/Mest imprinted gene on chromosome 6 identified by cDNA subtraction hybridization. Nat Genet 11, 52–59. https://doi.org/10.1038/ng0995-52.
Klenotic, P.A., Munier, F.L., Marmorstein, L.Y., Anand-Apte, B., 2004. Tissue inhibitor of metalloproteinases-3 (TIMP-3) is a binding partner of epithelial growth factor-containing fibulin-like extracellular matrix protein 1 (EFEMP1). Implications for macular degenerations. J Biol Chem 279, 30469–30473. https://doi.org/10.1074/jbc.M403026200.
Komander, D., Clague, M.J., Urbe, S., 2009. Breaking the chains: structure and function of the deubiquitinases. Nat. Rev. Mol. Cell Biol. 10, 550–563. https://doi.org/10.1038/nrm2731.
Kristiansen, H., Gad, H.H., Eskildsen-Larsen, S., Despres, P., Hartmann, R., 2011. The oligoadenylate synthetase family: an ancient protein family with multiple antiviral activities. J Interferon Cytokine Res 31, 41–47. https://doi.org/10.1089/jir.2010.0107.
Kwon, S.K., Saindane, M., Baek, K.H., 2017. p53 stability is regulated by diverse deubiquitinating enzymes. Biochim. Biophys. Acta Rev. Cancer 1868, 404–411. https://doi.org/10.1016/j.bbcan.2017.08.001.
Lai, K.P., Cheung, A.H.Y., Tse, W.K.F., 2017. Deubiquitinase Usp18 prevents cellular apoptosis from oxidative stress in liver cells. Cell Biol Int 41, 914–921. https://doi.org/10.1002/cbin.10799.
Li, B., Shin, J., Lee, K., 2009. Interferon-stimulated gene ISG12b1 inhibits adipogenic differentiation and mitochondrial biogenesis in 3T3-L1 cells. Endocrinology 150, 1217–1224. https://doi.org/10.1210/en.2008-0727.
Livak, K.J., Schmittgen, T.D., 2001. Analysis of relative gene expression data using real-time quantitative PCR and the 2(-Delta Delta C(T)) Method. Methods 25, 402–408. https://doi.org/10.1006/meth.2001.1262.
Madia, F., Worth, A., Whelan, M., Corvi, R., 2019. Carcinogenicity assessment: Addressing the challenges of cancer and chemicals in the environment. Environ Int 128, 417–429. https://doi.org/10.1016/j.envint.2019.04.067.
Malinowski, M., Pietraszek, K., Perreau, C., Boguslawski, M., Decot, V., Stoltz, J.F., Vallar, L., Niewiarowska, J., Cierniewski, C., Maquart, F.X., Wegrowski, Y., Brezillon, S., 2012. Effect of lumican on the migration of human mesenchymal stem cells and endothelial progenitor cells: involvement of matrix metalloproteinase-14. PLoS One 7, e50709. https://doi.org/10.1371/journal.pone.0050709.
Mari-Alexandre, J., Diaz-Lagares, A., Villalba, M., Juan, O., Crujeiras, A.B., Calvo, A., Sandoval, J., 2017. Translating cancer epigenomics into the clinic: focus on lung cancer. Transl Res 189, 76–92. https://doi.org/10.1016/j.trsl.2017.05.008.
Martelli, A., Rousselet, E., Dycke, C., Bouron, A., Moulis, J.M., 2006. Cadmium toxicity in animal cells by interference with essential metals. Biochimie 88, 1807–1814. https://doi.org/10.1016/j.biochi.2006.05.013.
Mashimo, T., Glaser, P., Lucas, M., Simon-Chazottes, D., Ceccaldi, P.E., Montagutelli, X., Despres, P., Guenet, J.L., 2003. Structural and functional genomics and evolutionary relationships in the cluster of genes encoding murine 2',5'-oligoadenylate synthetases. Genomics 82, 537–552.
Mastronardi, C., Whelan, F., Yildiz, O.A., Hannestad, J., Elashoff, D., McCann, S.M., Licinio, J., Wong, M.L., 2007. Caspase 1 deficiency reduces inflammation-induced brain transcription. Proc Natl Acad Sci U S A 104, 7205–7210. https://doi.org/10.1073/pnas.0701366104.
Mayer, W., Hemberger, M., Frank, H.G., Grummer, R., Winterhager, E., Kaufmann, P., Fundele, R., 2000. Expression of the imprinted genes MEST/Mest in human and murine placenta suggests a role in angiogenesis. Dev Dyn 217, 1–10.
McLaughlin, P.J., Bakall, B., Choi, J., Liu, Z., Sasaki, T., Davis, E.C., Marmorstein, A.D., Marmorstein, L.Y., 2007. Lack of fibulin-3 causes early aging and herniation, but not macular degeneration in mice. Hum Mol Genet 16, 3059–3070. https://doi.org/10.1093/hmg/ddm264.
Meplan, C., Verhaegh, G., Richard, M.J., Hainaut, P., 1999. Metal ions as regulators of the conformation and function of the tumour suppressor protein p53: implications for carcinogenesis. Proc Nutr Soc 58, 565–571.
Miller-Delaney, S.F., Lieberam, I., Murphy, P., Mitchell, K.J., 2011. Plxdc2 is a mitogen for neural progenitors. PLoS One 6, e14565. https://doi.org/10.1371/journal.pone.0014565.
Muro, R., Nitta, T., Kitajima, M., Okada, T., Suzuki, H., 2018. Rasal3-mediated T cell survival is essential for inflammatory responses. Biochem Biophys Res Commun 496, 25–30. https://doi.org/10.1016/j.bbrc.2017.12.159.
OECD, 2007. Detailed Review Paper on Cell Transformation Assays for Detection of Chemical Carcinogens. Development, O.f.e.c.-o.a. (Ed). OECD Environment, Health and Safety Publications. pp. 1–164.
Perelygin, A.A., Zharkikh, A.A., Scherbik, S.V., Brinton, M.A., 2006. The mammalian 2'-5' oligoadenylate synthetase gene family: evidence for concerted evolution of paralogous Oas1 genes in Rodentia and Artiodactyla. J Mol Evol 63, 562–576. https://doi.org/10.1007/s00239-006-0073-3.
Pluznick, J.L., Protzko, R.J., Gevorgyan, H., Peterlin, Z., Sipos, A., Han, J., Brunet, I., Wan, L.X., Rey, F., Wang, T., Firestein, S.J., Yanagisawa, M., Gordon, J.I., Eichmann, A., Peti-Peterdi, J., Caplan, M.J., 2013. Olfactory receptor responding to gut microbiota-derived signals plays a role in renin secretion and blood pressure regulation. Proc Natl Acad Sci U S A 110, 4410–4415. https://doi.org/10.1073/pnas.1215927110.
Pyakurel, A., Balmer, D., Saba-El-Leil, M.K., Kizilyaprak, C., Daraspe, J., Humbel, B.M., Voisin, L., Le, Y.Z., von Lintig, J., Meloche, S., Roduit, R., 2017. Loss of Extracellular Signal-Regulated Kinase 1/2 in the Retinal Pigment Epithelium Leads to RPE65 Decrease and Retinal Degeneration. Mol Cell Biol 37. https://doi.org/10.1128/MCB.00295-17.
Ray, P.D., Yosim, A., Fry, R.C., 2014. Incorporating epigenetic data into the risk assessment process for the toxic metals arsenic, cadmium, chromium, lead, and mercury: strategies and challenges. Front Genet 5, 201. https://doi.org/10.3389/fgene.2014.00201.
Ray, A.K., DuBois, J.C., Gruber, R.C., Guzik, H.M., Gulinello, M.E., Perumal, G., Raine, C., Kozakiewicz, L., Williamson, J., Shafit-Zagardo, B., 2017. Loss of Gas6 and Axl signaling results in extensive axonal damage, motor deficits, prolonged neuroinflammation, and less remyelination following cuprizone exposure. Glia 65, 2051–2069. https://doi.org/10.1002/glia.23214.
Redmond, T.M., Yu, S., Lee, E., Bok, D., Hamasaki, D., Chen, N., Goletz, P., Ma, J.X., Crouch, R.K., Pfeifer, K., 1998. Rpe65 is necessary for production of 11-cis-vitamin A in the retinal visual cycle. Nat Genet 20, 344–351. https://doi.org/10.1038/3813.
Saito, H., Kubota, M., Roberts, R.W., Chi, Q., Matsunami, H., 2004. RTP family members induce functional expression of mammalian odorant receptors. Cell 119, 679–691. https://doi.org/10.1016/j.cell.2004.11.021.
Schmidt, V., Schulz, N., Yan, X., Schurmann, A., Kempa, S., Kern, M., Bluher, M., Poy, M.N., Olivecrona, G., Willnow, T.E., 2016. SORLA facilitates insulin receptor signaling in adipocytes and exacerbates obesity. J Clin Invest 126, 2706–2720. https://doi.org/10.1172/JCI84708.
Silverman, R.H., Weiss, S.R., 2014. Viral phosphodiesterases that antagonize double-stranded RNA signaling to RNase L by degrading 2-5A. J Interferon Cytokine Res 34, 455–463. https://doi.org/10.1089/jir.2014.0007.
Smyth, G.K., 2004. Linear models and empirical bayes methods for assessing differential expression in microarray experiments. Stat. Appl. Genet. Mol. Biol. 3, Article3. https://doi.org/10.2202/1544-6115.1027.
Spiess, A.N., Walther, N., Muller, N., Balvers, M., Hansis, C., Ivell, R., 2003. SPEER–a new family of testis-specific genes from the mouse. Biol Reprod 68, 2044–2054. https://doi.org/10.1095/biolreprod.102.011593.
Suarez-Carmona, M., Lesage, J., Cataldo, D., Gilles, C., 2017. EMT and inflammation: inseparable actors of cancer progression. Mol Oncol 11, 805–823. https://doi.org/10.1002/1878-0261.12095.
Suzuki, R., Matsumoto, M., Fujikawa, A., Kato, A., Kuboyama, K., Yonehara, K., Shintani, T., Sakuta, H., Noda, M., 2014. SPIG1 negatively regulates BDNF maturation. J Neurosci 34, 3429–3442. https://doi.org/10.1523/JNEUROSCI.1597-13.2014.
Tang, L., Qiu, R., Tang, Y., Wang, S., 2014. Cadmium-zinc exchange and their binary relationship in the structure of Zn-related proteins: a mini review. Metallomics 6, 1313–1323. https://doi.org/10.1039/c4mt00080c.
Thevenod, F, 2010. Catch me if you can! Novel aspects of cadmium transport in mammalian cells. Biometals 23, 857–875. https://doi.org/10.1007/s10534-010-9309-1.
Timpl, R., Sasaki, T., Kostka, G., Chu, M.L., 2003. Fibulins: a versatile family of extracellular matrix proteins. Nat. Rev. Mol. Cell Biol. 4, 479–489. https://doi.org/10.1038/nrm1130.
Tonami, K., Kurihara, Y., Arima, S., Nishiyama, K., Uchijima, Y., Asano, T., Sorimachi, H., Kurihara, H., 2011. Calpain-6, a microtubule-stabilizing protein, regulates Rac1 activity and cell motility through interaction with GEF-H1. J Cell Sci 124, 1214–1223. https://doi.org/10.1242/jcs.072561.
Urani, C., Stefanini, F.M., Bussinelli, L., Melchioretto, P., Crosta, G.F., 2009. Image analysis and automatic classification of transformed foci. J Microsc 234, 269–279. https://doi.org/10.1111/j.1365-2818.2009.03171.x.
Urani, C., Melchioretto, P., Bruschi, M., Fabbri, M., Sacco, M.G., Gribaldo, L., 2015. Impact of Cadmium on Intracellular Zinc Levels in HepG2 Cells: Quantitative Evaluations and Molecular Effects. Biomed Res Int 2015, 949514. https://doi.org/10.1155/2015/949514.
Vakilian, A., Khorramdelazad, H., Heidari, P., Sheikh Rezaei, Z., Hassanshahi, G., 2017. CCL2/CCR2 signaling pathway in glioblastoma multiforme. Neurochem Int 103, 1–7. https://doi.org/10.1016/j.neuint.2016.12.013.
Vanparys, P., Corvi, R., Aardema, M.J., Gribaldo, L., Hayashi, M., Hoffmann, S., Schechtman, L., 2012. Application of in vitro cell transformation assays in regulatory toxicology for pharmaceuticals, chemicals, food products and cosmetics. Mutat Res 744, 111–116. https://doi.org/10.1016/j.mrgentox.2012.02.001.
de Vega, S., Iwamoto, T., Nakamura, T., Hozumi, K., McKnight, D.A., Fisher, L.W., Fukumoto, S., Yamada, Y., 2007. TM14 is a new member of the fibulin family (fibulin-7) that interacts with extracellular matrix molecules and is active for cell binding. J Biol Chem 282, 30878–30888. https://doi.org/10.1074/jbc.M705847200.
de Vega, S., Iwamoto, T., Yamada, Y., 2009. Fibulins: multiple roles in matrix structures and tissue functions. Cell Mol Life Sci 66, 1890–1902. https://doi.org/10.1007/s00018-009-8632-6.
Virani, S., Rentschler, K.M., Nishijo, M., Ruangyuttikarn, W., Swaddiwudhipong, W., Basu, N., Rozek, L.S., 2016. DNA methylation is differentially associated with environmental cadmium exposure based on sex and smoking status. Chemosphere 145, 284–290. https://doi.org/10.1016/j.chemosphere.2015.10.123.
Volpe, M., Shpungin, S., Barbi, C., Abrham, G., Malovani, H., Wides, R., Nir, U., 2006. trnp: A conserved mammalian gene encoding a nuclear protein that accelerates cell-cycle progression. DNA Cell Biol 25, 331–339. https://doi.org/10.1089/dna.2006.25.331.
Vukovic, J., Marmorstein, L.Y., McLaughlin, P.J., Sasaki, T., Plant, G.W., Harvey, A.R., Ruitenberg, M.J., 2009. Lack of fibulin-3 alters regenerative tissue responses in the primary olfactory pathway. Matrix Biol 28, 406–415. https://doi.org/10.1016/j.matbio.2009.06.001.
Wang, J., Duncan, D., Shi, Z., Zhang, B., 2013. WEB-based GEne SeT AnaLysis Toolkit (WebGestalt): update 2013. Nucleic Acids Res 41, W77–83. https://doi.org/10.1093/nar/gkt439.
Way, G., Morrice, N., Smythe, C., O'Sullivan, A.J., 2002. Purification and identification of secernin, a novel cytosolic protein that regulates exocytosis in mast cells. Mol Biol

Cell 13, 3344–3354. https://doi.org/10.1091/mbc.e01-10-0094.
Wilde, E.C., Chapman, K.E., Stannard, L.M., Seager, A.L., Brusehafer, K., Shah, U.K., Tonkin, J.A., Brown, M.R., Verma, J.R., Doherty, A.T., Johnson, G.E., Doak, S.H., Jenkins, G.J.S., 2018. A novel, integrated in vitro carcinogenicity test to identify genotoxic and non-genotoxic carcinogens using human lymphoblastoid cells. Arch Toxicol 92, 935–951. https://doi.org/10.1007/s00204-017-2102-y.
Wolter, J., Schild, L., Bock, F., Hellwig, A., Gadi, I., Al-Dabet, M.M., Ranjan, S., Ronicke, R., Nawroth, P.P., Petersen, K.U., Mawrin, C., Shahzad, K., Isermann, B., 2016. Thrombomodulin-dependent protein C activation is required for mitochondrial function and myelination in the central nervous system. J Thromb Haemost 14, 2212–2226. https://doi.org/10.1111/jth.13494.
Yoshimura, T, 2018. The chemokine MCP-1 (CCL2) in the host interaction with cancer: a foe or ally? Cell Mol. Immunol. 15, 335–345. https://doi.org/10.1038/cmi.2017.135.
Zhang, R., Pan, X., Huang, Z., Weber, G.F., Zhang, G., 2011. Osteopontin enhances the expression and activity of MMP-2 via the SDF-1/CXCR4 axis in hepatocellular carcinoma cell lines. PLoS One 6, e23831. https://doi.org/10.1371/journal.pone.0023831.
Zhang, H., Kho, A.T., Wu, Q., Halayko, A.J., Limbert Rempel, K., Chase, R.P., Sweezey, N.B., Weiss, S.T., Kaplan, F., 2016. CRISPLD2 (LGL1) inhibits proinflammatory mediators in human fetal, adult, and COPD lung fibroblasts and epithelial cells. Physiol. Rep. 4. https://doi.org/10.14814/phy2.12942.
Zhao, H., Chen, Q., Alam, A., Cui, J., Suen, K.C., Soo, A.P., Eguchi, S., Gu, J., Ma, D., 2018. The role of osteopontin in the progression of solid organ tumour. Cell Death Dis 9, 356. https://doi.org/10.1038/s41419-018-0391-6.